P. K. Pepeljugoski D. M. Kuchta

Design of optical communications data links

This paper is primarily an overview of data link design efforts in IBM pertinent to local area networks (LANs) using both multimode fiber (MMF) and single-mode (SMF) links, with emphasis on MMF links operating at short wavelengths. Device models (laser and receiver) and multimode fiber models are discussed, as well as noise aspects (modal and mode partition noise). In addition, new simulation and measurement results for a 20-Gb/s 1-km-long link are presented.

Introduction

Prior to the development of the Fibre Channel and Gigabit Ethernet² standards in the mid-1990s, multimode fiber link design was based on the use of light-emitting diodes (LEDs). Their use permitted easy characterization of the fiber's major property, bandwidth, which was assumed to be at its minimum level. The low data rates of 125 Mb/s [Fiber Distributed Data Interface (FDDI) data rate] and 200 Mb/s [Enterprise Systems Connection (ESCON*) data rate [1] permitted the assumption that all worst-case conditions could occur simultaneously and the link would still work with an adequate margin. With the need for data rates greater than 1 Gb/s, continued use of minimum fiber bandwidth and simultaneous worst-case conditions would have resulted in links with distance limits so short (e.g., 125 m, which was once proposed as the maximum distance for the Gigabit Ethernet 62.5-µm fiber solution) as to render the solution useless or at least unmarketable. Improved link modeling and the use of statistics were needed to restore the multimode fiber solution. This paper discusses the link modeling and models used by IBM to influence international standards such as Fibre Channel, Gigabit Ethernet, and asynchronous transfer mode (ATM).

The design of communication links for LAN applications, such as Ethernet and Fibre Channel, differs significantly from the design of long-haul telecommunication links. The primary factor affecting their design is the overall cost of the components of the links. This dictates

all other choices made in the link design. For example, multimode fiber is used for the vast majority of the LAN links. While multimode fiber is unable to reach the distances achieved with single-mode fiber, it offers significant savings in the design of the transmitter and the receiver. Because of the size of the multimode fiber core, the placement tolerances of the laser and the lens relative to the fiber in the transmitter are greatly relaxed, permitting passive alignment and resulting in reduced assembly costs. Furthermore, inexpensive materials such as plastics can be used for some of the components, further reducing the cost. In addition, 850-nm vertical-cavity surface-emitting lasers (VCSELs) are used in the vast majority of newly installed LAN links because of their cost advantage.

There are several commercial products which permit users to simulate optical links, mostly targeting telecommunication links. Because of their limited capabilities and the inability to simulate multimode fiber links, companies designing and developing LAN products have used their internal tools or simple spreadsheet-based link models that were tailored for LED-driven links [2]. The use of simulation tools was accelerated in the mid-1990s in the midst of an environment of reduced development time and strict requirements regarding link failure rates. The developers, both transceiver and fiber manufacturers, had to perform thorough exploration of the parameter space, which was achievable only by a combination of large-scale simulations and a limited set of critical laboratory experiments.

This paper is divided into three sections. In the first section, we discuss the approach to modeling and simulation used in an IBM simulation tool to design LAN

©Copyright 2003 by International Business Machines Corporation. Copying in printed form for private use is permitted without payment of royalty provided that (1) each reproduction is done without alteration and (2) the *Journal* reference and IBM copyright notice are included on the first page. The title and abstract, but no other portions, of this paper may be copied or distributed royalty free without further permission by computer-based and other information-service systems. Permission to *republish* any other portion of this paper must be obtained from the Editor.

0018-8646/03/\$5.00 © 2003 IBM

¹ ANSI/INCITS, Technical Committee T11, American National Standards Institute and International Committee for Information Technology Standards, Washington, DC, 1992.

² IEEE Standard 802.3, Institute of Electrical and Electronics Engineers, New York, NY, 1997.

links. In the next section, we describe the device and noise models implemented in the simulation tool. In the final section, we present a few examples of LAN link design for which cost considerations determined the choices of the link parameters and the use of the models and methodology described in the first and the second sections was crucial.

Simulation methodology

Simulation approach

The development of the simulation methodology depends on several factors: target environment [i.e., LAN, telecommunication links, or computer interconnections (referred to as *interconnects*)]; desired accuracy (in some cases link overdesign is acceptable); time required to generate simulation outputs (on some occasions the output should be immediate); and an acceptable level of complexity and input parameters (the operator is sometimes the designer of a particular component, and sometimes a standards user). The requirements for parallel links and interconnects differ from those of LANs. For example, interconnect requirements include component variation that must be addressed in a statistical manner. However, even for interconnects, there is a difference between in-the-box applications and those for parallel links for distances up to several hundred meters. The initial methodology and models reported here were first implemented and tested in an IBM internal simulation tool designated OBST (Optical Bus Simulation Tool), a MATLAB**-based3 CAD tool for parallel optical interconnects used in the Optoelectronic Technology Consortium (OETC) [3] bus design. It was later implemented in the iFROST CAD tool for optical interconnects [4, 5]. The models, in particular those relevant to multimode fiber links, and the performance evaluation methodology were later modified to apply to the serial links that pertain to the IEEE 802.3z (Gigabit Ethernet) and Fibre Channel standards. The MATLABbased tool has evolved into what is subsequently referred to as the "IBM optical link simulator."

There are several types of analysis results that are desirable from the simulation of an optical link; these include signal waveforms, eye diagrams, deterministic and random jitter, and signal-to-noise ratios (SNRs). Parallel links require additional outputs such as the bit error ratio (BER) vs. the timing offset from the reference sampling time for synchronous buses. To obtain these analysis results, it is necessary to perform a waveform simulation which takes into account the various signal degradation mechanisms that affect the eye diagram and BER of the

bus. These mechanisms include statistical variation in component parameters, launch conditions, deterministic and random jitter, skew, laser mode structure, laser relaxation oscillations, dispersion, attenuation, crosstalk, and noise. Although the discussion that follows applies to single-channel links, the simulations approach can easily be modified to apply to parallel links (either in space or wavelength domain).

Sources of performance degradation

In a serial link, the simulation parameters for each of the components have a certain manufacturing distribution. This variation in component parameters results in variability in the link power budget. The challenge is to identify the mean and standard deviations of these distributions, and to evaluate the link performance in a statistical manner so that there is no overdesign of the link. For example, if a particular worst-case component parameter results in a 1-dB power penalty and the probability of obtaining that component is, for example, 10^{-7} , this becomes a nonissue, since the failure rate is very low when considering the entire space of parameters in the simulation.

Besides the variation in the component parameters between the channels, there are the inevitable changes due to laser launch conditions, timing jitter in the transmitter driving electronics, and timing jitter due to the pattern-dependent laser turn-on delay. While these effects individually may be considered negligible, when combined they can significantly increase the total penalties in the link. An even larger potential problem in the optical interconnect environment is that the variations in laser threshold currents within the laser diode array can lead to high variation in the pattern-dependent laser turn-on delays. This is particularly important in an environment in which the bit pattern run length is not bounded.

Computational efficiency and simulation methodologies

To perform a link failure rate analysis, a statistical analysis is performed in which the link parameters (simulation inputs) are treated as independent members of a statistical ensemble. The link parameters are considered to be time-invariant independent random variables and are chosen at the beginning of the simulation run. Once chosen, the link parameters are treated as deterministic throughout the simulation. The probability distribution functions for these random variables are based on measurements and estimates. Multiple simulations can be performed with randomized parameter values and their results used together to obtain a more accurate prediction of how the performance of the link is affected by the statistical variation in component parameters. Consequently, there is a tradeoff between computation

³ MATLAB is a product of The MathWorks, Inc., 24 Prime Park Way, Natick, MA 01760.

time and accuracy of the results. The efficiency of the simulation is improved by choosing a distribution for the parameter variations that provides an even sampling of the value range. Therefore, in performing the simulations, it is desirable to take a moderately conservative approach and simulate the performance in the presence of the full range of expected component variations.

The need to perform a large number of simulations while varying component parameters according to their statistical distributions in turn requires that each simulation be performed in the most time-efficient manner possible. To maximize computational efficiency, it is helpful to consider the efficiency of noiseless signal simulation and the efficiency of the treatment of noise in the simulation as separate aspects [6]. The use of a mixed-level simulation approach minimizes the computational requirements of the simulation of the noiseless waveform. In a mixed-level simulation approach, each component is modeled independently at a level of abstraction that minimizes the computational requirements for the simulation while attaining the required simulation accuracy and precision.

For the minimization of the computational requirements for the treatment of noise, the quasi-analytical approach is used for simulation and analysis of the OETC optical bus and the subsequent applications of the program to Ethernet and Fibre Channel serial links. In the quasianalytical approach, use is made of a hybrid of simulation and analysis in which the system simulation is divided between the simulation of noiseless signal waveforms and analysis of the noise [5]. Simulation begins by generating noiseless waveforms at the link data input and proceeds through each subsequent component model until the system output is generated. The noise is separately computed using analytical equations. Signal-dependent noise, such as mode partition noise, may be based on the input of some of the signal waveforms at the driven device output. The contributions from the different noise sources (thermal noise, shot noise, etc.) are accumulated, and the total equivalent output noise is calculated. At this point, a formula uses the simulated signal waveform and the calculated noise power to compute the probability of error, given the probability density function of the noise.

The quasi-analytical approach takes into account, to the level of accuracy permitted by the device models, various signal degradations and distortions that occur through the signal propagation in the system. These signal degradations are translated to degradations in the eye diagram and change in the signal magnitude at the decision sampling time. Since the noise is separately calculated, no effects of the noise are shown in the signal waveforms. The degradations that affect both signal and noise power, such as attenuation in the fiber, are also

taken into account in the computation of the noise through the system. This approach is valid as long as the noise in the system does not experience nonlinear distortions and the noise probability density function is known

The formula used to compute the BER from the simulated signal and calculated noise power is determined by the noise distribution. If it is assumed that the noise has a Gaussian distribution,

$$BER = \frac{1}{N} \sum_{i=1}^{N} \left[0.5 erfc \left(\frac{V_i - V_{th}}{\sqrt{2}\sigma_1} \right) u(V_i - V_{th}) \right.$$

$$\left. + 0.5 erfc \left(\frac{V_{th} - V_i}{\sqrt{2}\sigma_0} \right) u(V_{th} - V_i) \right], \qquad (1)$$

where u(x) is the Heaviside step function defined as u(x)=1 if $x\geq 0$ and 0 if x<0, V_i and $V_{\rm th}$ are the signal values and the decision threshold at the decision sample times (for ac-coupled designs, $V_{\rm th}=0$), and σ_0 and σ_1 are the noise standard deviation values for the 0 bit and the 1 bit, respectively; N is the total number of bits in the simulated bit sequence.

The calculation of the BER takes into account the signal degradations that occur during link propagation. These degradations are due to the finite rise/fall times at the driver circuits and the laser, fiber dispersion and/or the finite modal bandwidth of the multimode fiber, and the receiver transimpedance amplifier (TIA) and postamplifier. The deterministic jitter, which is defined as the pattern-dependent horizontal eye closure at the threshold level, can be calculated directly from the signal waveform and/or by calculating the BER as a function of sampling time, resulting in a "bathtub-like" curve.

In a statistical computation, one can calculate the probability of an error based on a set of randomly selected simulation inputs drawn from the given distribution of component parameters. Then, the simulation is repeated for a very large number of links, and a histogram of the overall link performance is generated. Usually, for Ethernet LAN links, it is acceptable if <1% of all links fail when all component parameters are at their worst-case value, with the exception of one, which may exceed that value. The failure of the link is defined as an event for which the total penalties are higher than the available margin, or jitter exceeding the specifications, leading to a BER value that is greater than required, but not unavailability of the link. It is worth emphasizing here the distinction between the failure rate defined here to represent reduced performance and the outage, which represents total unavailability of the channel for data transmission during a period of time. From the available simulation outputs [intersymbol interference (ISI) penalty, available margin, deterministic jitter (DJ), or retiming

 Table 1
 Laser model parameter definitions.

Parameter	Definition
N	Number of electrons in the active region
n	Carrier density = N/V
P	Number of photons in the lasing mode
$G = \Gamma v_{\rm g} a (N - N_{\rm o})$	Net rate of stimulated emission
Γ	Mode confinement factor
$ u_{ m g}$	Velocity of light in the laser medium
a	Differential gain constant
$N_{ m o}$	Carrier number required to achieve transparency
V	Volume of the laser cavity
$lpha_{ m m}$	Mirror losses
$lpha_{ m int}$	Internal losses
$oldsymbol{eta}_{ m sp}$	Fraction of spontaneous emission coupled into the lasing mode
ε	Gain nonlinearity factor
A	Nonradiative recombination rate
B	Radiative recombination rate (bimolecular recombination)
C	Auger recombination coefficient

window], one can select the specifications for the link parameters until the desired failure rate is met. This usually means tweaking of a particular parameter to optimize cost benefits.

Link component models

This section details the deterministic models that are used for the three basic link devices: the optical source, the fiber, and the optical detector.

Laser model

The need for an accurate laser model arises in at least two instances: one for link simulation and the other for the optimized design of an integrated circuit to drive the laser. For the former, a time domain transfer function model would suffice; however, for the latter the temperature dependence of the laser becomes important, and an accurate input impedance model is also required. Because the current data rates of interest are greater than 1 Gb/s, in both cases the time domain transfer function must be described by nonlinear laser rate equations. There are many sources of laser rate equations in the literature; in this paper we use the notation found in [7].

The single-mode laser rate equations are actually a pair of coupled differential equations, one pertaining to the number of electrons N [Equation (2)] and the other to the number of photons in the lasing mode P [Equation (3)]. The parameters used are defined in **Table 1**. These rate

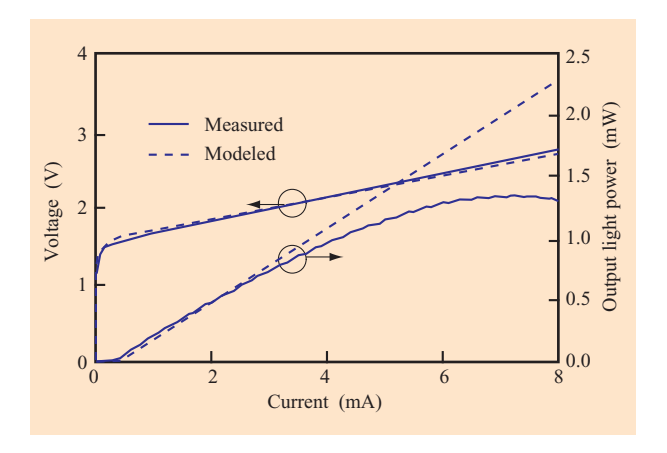
equations are the same as those based on electron and photon densities, except that both sides have been multiplied by the cavity volume of the laser. They have also been modified by the inclusion of a gain nonlinearity factor $1 - \varepsilon P$, which is used to characterize the combined effects of gain saturation and lateral carrier diffusion [8]. The modified equations are

$$\frac{dN}{dt} = \frac{I}{q} - (A + Bn + Cn^2)N - \Gamma \nu_{\rm g} a(N - N_0)P(1 - \varepsilon P)$$
(2)

and

$$\frac{dP}{dt} = \left[\Gamma \nu_{\rm g} a (N - N_0) P (1 - \varepsilon P) - \nu_{\rm g} (\alpha_{\rm m} + \alpha_{\rm int})\right] + \beta_{\rm sp}^2 N^2 V. \tag{3}$$

A laser model based on temperature-dependent rate equations had been developed [9] in which the temperature dependence was empirically assigned to N_0 and a. This same temperature dependence was incorporated into the laser model described here by assuming that $a(T) = a_0 \exp(-T/T_0)$ and $N_o(T) = N_{o0} \exp(T/T_0)$, where T_0 is the characteristic temperature of the laser and a_0 and N_{o0} are the values of a and N_o at T=0°C. Although temperature dependence is included, this is a static temperature, and thus effects such as dynamic junction heating are not included.



Comparison of experimental and predicted dc current sweep behavior for an 850-nm VCSEL. The predicted behavior was obtained using a rate-equation-based model. The deviation in the light power curve above 3 mA was attributed to junction heating.

For simulations with a real driver circuit, these rate equations are converted to an equivalent circuit following the methodology used in [10]. Several changes are made to the model used in [10], most notably the inclusion of the gain nonlinearity factor and the assumption of linear rather than parabolic gain. One advantage of the circuit form of the laser model is that the device and package parasitics are easily incorporated as additional circuit elements.

It should be noted that these rate equations are single-mode rate equations. Multimode rate equations are a straightforward extension. Although all of the lasers used in the 850-nm wavelength range with multimode fiber are multimode lasers, including VCSELs, the single-mode rate equations have been found to provide a very good approximation for large-signal behavior and have the added benefit of simplicity, relatively short computation times, and fewer convergence problems.

Illustrative use of the laser model

Before the model can be used, the model parameters must be extracted from a series of ac and dc measurements performed on an actual device. However, not all of the parameters can be directly measured. Those that cannot be measured are either supplied by the manufacturer or are estimated and adjusted until a reasonable fit between the model and measurement is obtained. Illustratively, **Figure 1** pertains to use of the laser model [Equations (2) and (3) with time derivatives set to 0] in a simulation of the dc laser properties of a VCSEL. The measured and predicted current–voltage (*I–V*) characteristics were in good agreement. The emission characteristics were in

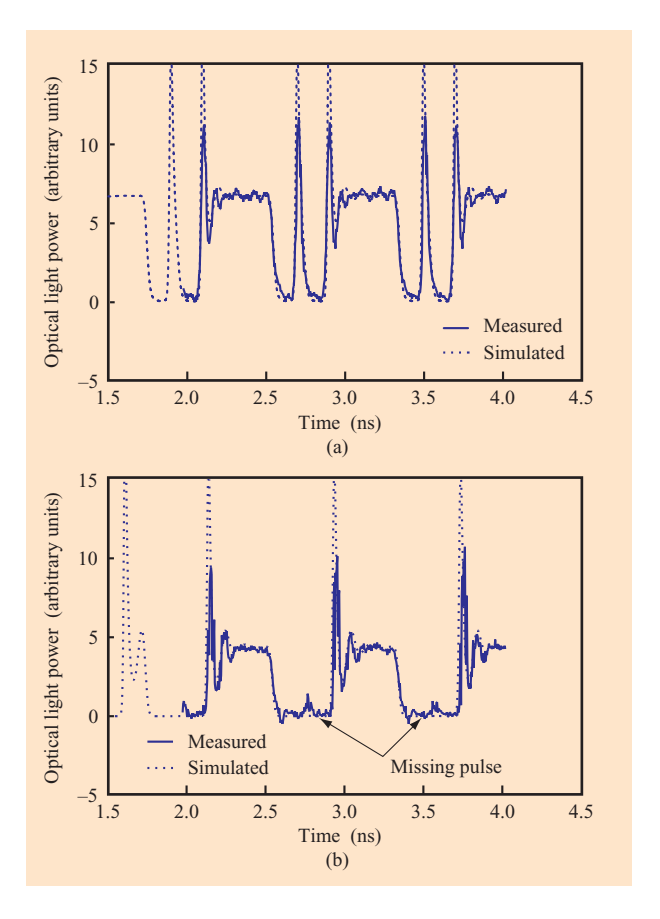
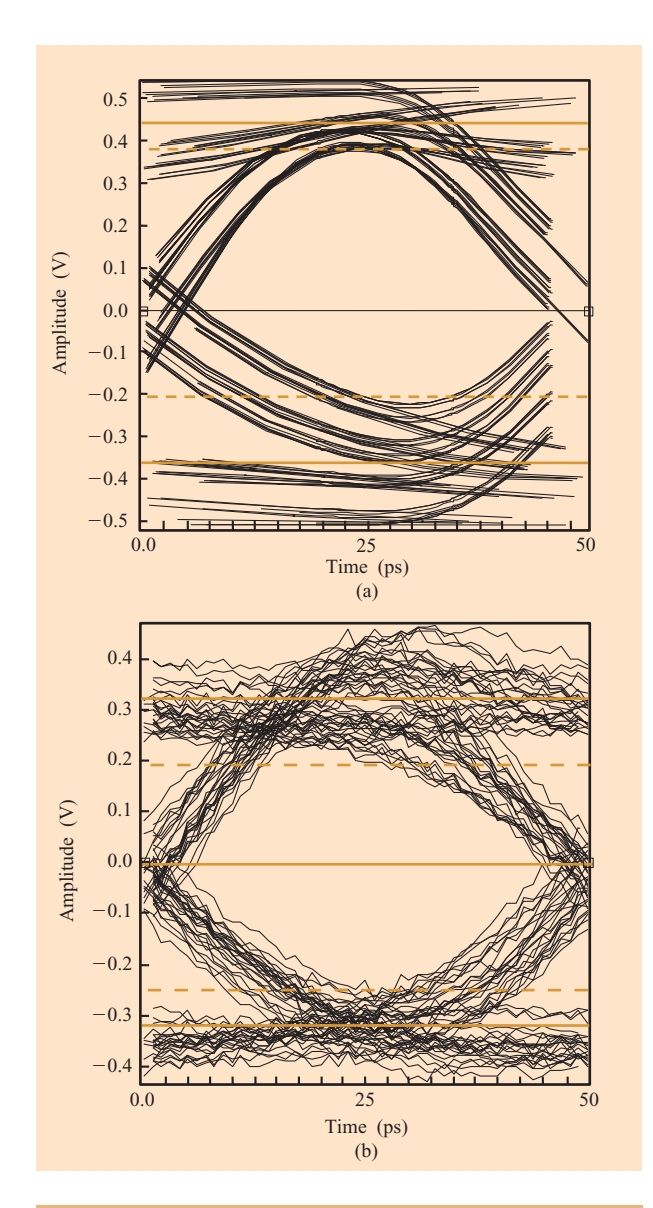


Figure 2

Comparison of predictions based on the laser model with measurements under ac conditions. In (a), a 10-Gb/s waveform was used with the laser biased above threshold. In (b), a 10-Gb/s pattern was used with the laser biased sufficiently below threshold in the low level to cause the isolated 1 in the waveform to disappear (see missing pulse regions).

good agreement from 0 to 3 mA and then started to deviate. This deviation was attributed to junction heating in the VCSEL. It was acceptable since the ac slope of the output light power curve did not follow the dc slope and was actually much closer to the slope in the model.

Figure 2(a) shows an illustrative comparison with measurement under ac conditions. The laser was biased above threshold at all times in this measurement. Results were in fairly good agreement with the model, although the model exhibited more overshoot on the rising edge and a slightly faster fall time. Both of these differences could be improved by further adjustment of the parameters. A good test of any laser model is one that demonstrates its nonlinearity when the laser is biased from below threshold. In a below-threshold condition, the laser exhibits a turn-on delay. If the bias level of the state is lowered sufficiently, the turn-on delay can exceed a bit



(a) Predictions from laser model simulation of a VCSEL driven with a data pattern at 20 Gb/s; simulated intersymbol interference (ISI) and simulated deterministic jitter (DJ) were found to be 1.43 dB and 11.6 ps, respectively. (b) Experimental results for a VCSEL operating at 20 Gb/s at an ISI of 1.63 dB and a DJ of 14.2 ps.

period (100 ps for 10 Gb/s), and isolated 1s in the pattern will disappear entirely. **Figure 2(b)** shows a comparison of a measurement for which the 0 level of the laser was adjusted until the isolated 1 in the pattern had almost entirely disappeared, and the corresponding simulation of this condition. In this simulation, the model parameters were the same as those of Figure 2(a); only the driving currents were adjusted. The model predicts that the isolated 1 should disappear sooner

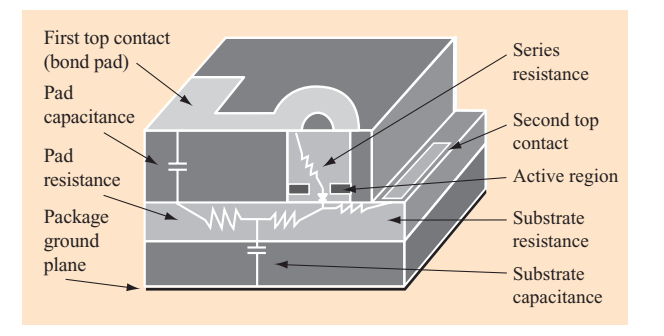


Figure 4

Cross section of a typical VCSEL; also depicted are its major parasitic elements.

than it does in the measurement, resulting in a conservative prediction.

Figure 3 illustrates another use of the model in predicting record high-speed modulation of a VCSEL at 20 Gb/s. Figure 3(a) shows a simulated eye diagram at 20 Gb/s from the model of Figure 1 with no change in parameters, while Figure 3(b) shows the measured result at 20 Gb/s [11]. The measured values of intersymbol interference (ISI) and deterministic jitter (DJ) were close to but slightly higher than the predicted values. The difference was attributed to the following: In the simulation, the source DJ was zero, and the use of a detector having an infinite bandwidth was assumed.

Impedance modeling: Laser model with parasitic elements

The use of the equivalent-circuit form of the laser model [10] in combination with device parasitic elements for simulations with a real driver circuit was mentioned earlier. To properly design a driver circuit for maximum power transfer of signals having fast edges, it is necessary to have a good model for the load, which in this case is a laser diode. Figure 4 shows a cross section of a typical VCSEL and identifies its major parasitic elements. The latter are its series resistance, which consists of upper and lower mirror components, its the bond pad capacitance, the substrate resistance, and an additional substrate capacitance for VCSELs fabricated with a semi-insulating substrate and then packaged over a ground plane. Not shown in the figure is the depletion capacitance. The diffusion capacitance is contained within the carrier rate equation of the VCSEL. The parasitic elements can be extracted from its dc I-V curves, capacitance vs. voltage curves, and network analyzer measurements vs. bias.

Figure 5 shows the measured and predicted input impedance (shown as the network scattering parameter

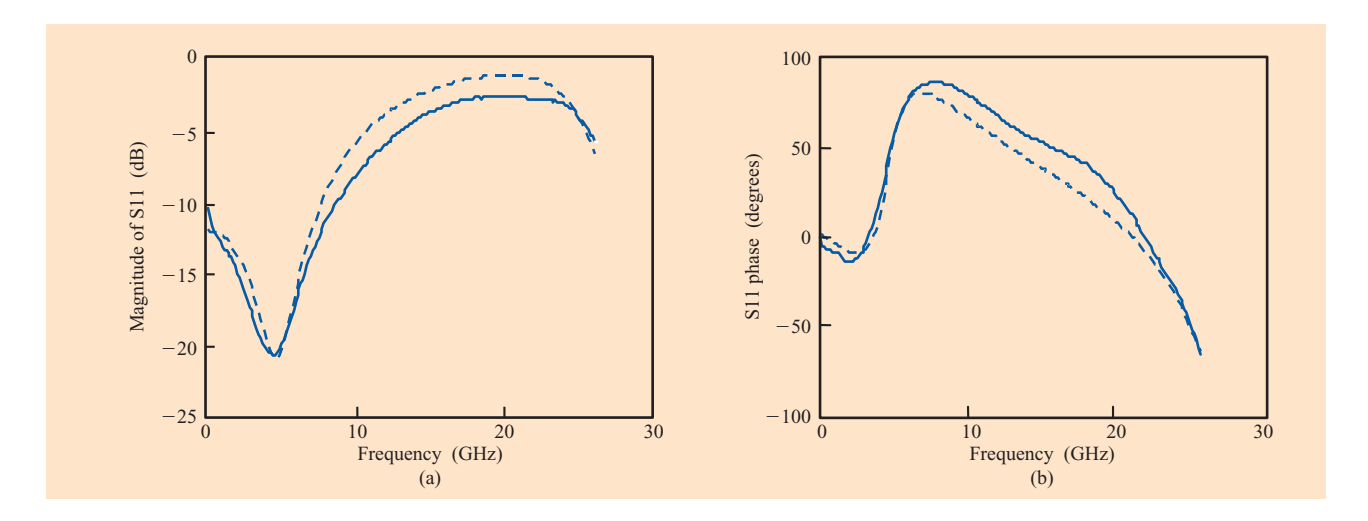


Figure 5

Measured (solid curve) and predicted (dashed curve) frequency dependence of the S11 of a typical VCSEL: (a) Magnitude; (b) phase.

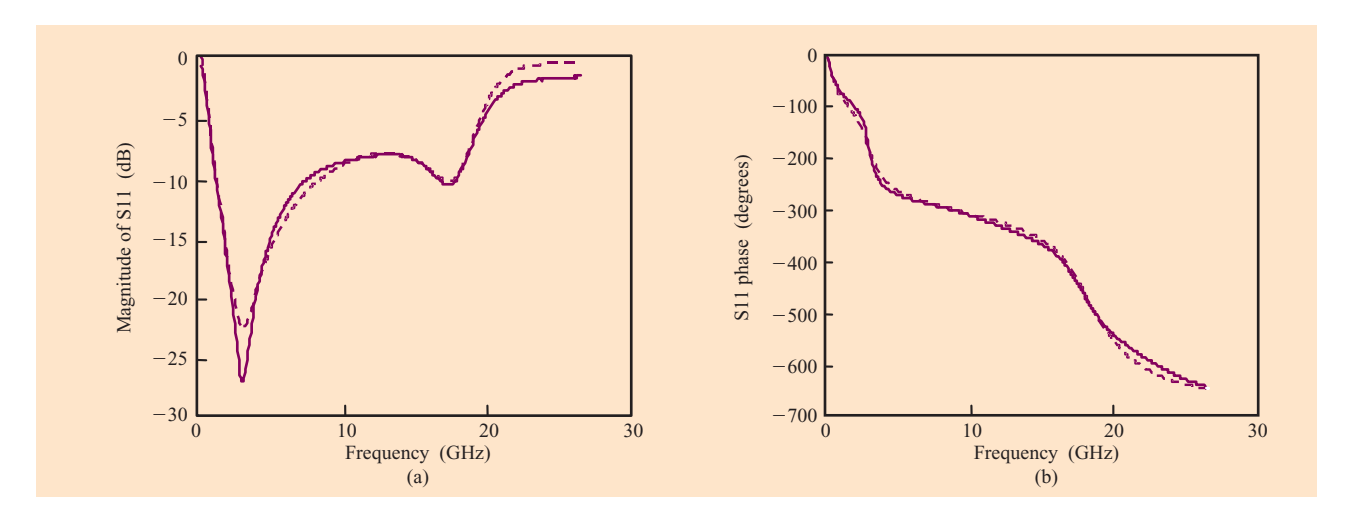


Figure 6

Measured (solid curve) and predicted (dashed curve) frequency dependence of the S11 of a laser with a matching resistor: (a) Magnitude; (b) phase.

S11) of a typical VCSEL. Since the impedance is complex, it is necessary to depict either its real and imaginary parts or its magnitude and phase. In this case the magnitude and phase are shown. The agreement between measured and predicted behavior was better than 20% over the frequency range from 40 MHz to 26 GHz. **Figure 6** shows another example of laser impedance modeling. In this example, the laser was packaged with a chip resistor to attempt to match the impedance to a $50-\Omega$ transmission

line. The low-frequency value of S11 was near 0 dB because the laser was not biased during measurement.

Receiver model

The receiver has two blocks: the first consists of the photodiode (PD) and the transimpedance amplifier (TIA), and the second consists of the postamplifier (PA). The role of the photodiode and the TIA is to convert the optical signal into an electrical signal, with a minimum

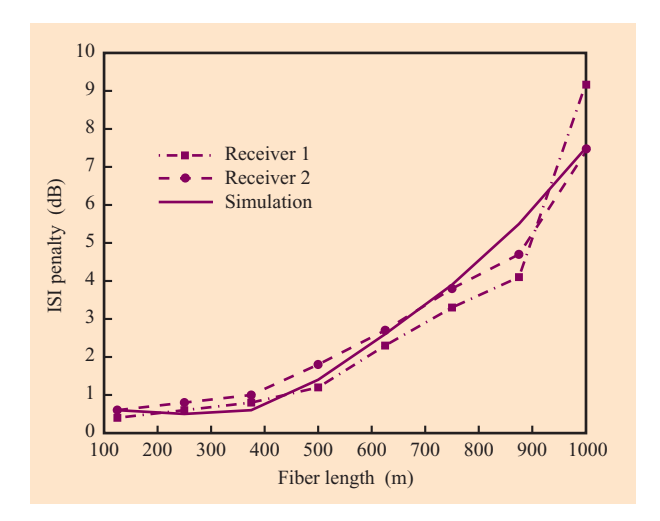


Figure 7

Comparison of predicted and measured ISI penalty for a Gigabit Ethernet link for two slightly different receivers.

of added noise. The signal at the TIA output may be saturated. If the signal was weak and saturation does not occur at the TIA output, the postamplifier amplifies the signal to levels that represent the logical 1s and 0s.

The model for the photodiode and the TIA is the same as the one described in [4]. The postamplifier is modeled as a low-pass Butterworth filter with given order N. Typical values for N are 2–4. **Figure 7** shows a comparison of ISI penalty simulations of the preamplifier section of the receiver modeled within MATLAB (modeled as a fourth-order Butterworth filter) and implemented as a real circuit in HSPICE** using the same input signal. The simulations showed very good agreement when a signal with worst-case ISI values was presented at the input.

Fiber model

In Ethernet and Fibre Channel applications, the majority of link lengths are less than 300 m, and the maximum distances for premises wiring are up to 550 m. In this environment, the 62.5- μ m core fiber had, for a considerable time, sufficient bandwidth to cover the premises distances and beyond. However, the advent of the laser-driven gigabit LAN links exposed the variability of the bandwidth of the multimode fibers and the need for extension of the achievable distances in those standards. To develop the next-generation multimode fiber, accurate models for laser-driven links were needed.

Several models for multimode fibers have been described in the literature. The fiber is usually modeled as a low-pass filter with a bandwidth that can be determined from the overfilled bandwidth. The LAN standards are

based on the simplest approach, involving the assumption that the transfer function of the fiber and every other component in the link is Gaussian. While this approach works well for LED-driven links, for laser diodes and multimode fiber links a more accurate approach must be adopted, since the laser beam size and numerical aperture affect the bandwidth of the fiber.

In a multimode fiber, the light propagates in a number of mode groups that travel in the fiber with different velocities, giving rise to intermodal dispersion. The modal bandwidth of the fiber, resulting from the intermodal dispersion, depends on launch conditions. Those conditions determine the amount of power launched into each of the mode groups, and, together with mode delays, determine the transfer function of the fiber. The mode delays can be calculated for a known fiber profile using the scalar wave equation [12]. Similarly, one can compute the coupling coefficients (the fraction of total optical power launched into mode group) using the overlap integral [13]. In that case, and in the ideal case corresponding to the absence of offset in the connectors, the transfer function is given by

$$H(jf) = \sum_{k=1}^{M} w_k \exp(-2\pi j f \tau_k), \tag{4}$$

where w_k are the weighting factors and τ_k are delay times of each mode. The weighting factors take into account how much power is launched into each mode (group) and how much each mode (group) is attenuated during the transmission. Without loss of generality, and to gain better insight into the problem, we assume that the mode attenuation is uniform; i.e., it is the same for all modes. Also, for the fiber lengths of interest it can be assumed that there is no mode coupling.

In practice, real connectors have an offset with respect to one another, so they introduce mode mixing, which affects the transfer function of the fiber. At a connector, first there is redistribution of the optical power in the mode group, and second, there is distortion because the modes are delayed with respect to one another when they reach the connector. The redistribution of power at the connector can be described by connector transfer matrix C with elements $c_{i,k}$, whose size is $M \times M$, where M is the number of mode groups. The calculation of elements of the connector transfer matrix for a given connector offset is straightforward but time-consuming, and is performed by computing the overlap integral of the spatial fields of the fiber modes in each fiber. If the source has a mode power distribution at the fiber input given by a vector P_{a} (and elements p_{ν}), the frequency domain representation of the signal at the first connector input is given by

$$Y_{c}(f) = \sum_{q=1}^{M} Y_{q} = \sum_{q=1}^{M} p_{q} \exp[-j\omega t_{q}L]X(f),$$
 (5)

where X(f) is the frequency domain representation of the signal at the input of the fiber. Then the signal at the connector output is given by

$$Y_{\text{co},q}(f) = \sum_{i=1}^{M} c_{j,q} Y_j(f),$$
 (6)

where $q=1, 2, \cdots, M$ denotes the fiber mode groups. The fiber transfer function, needed to calculate the fiber bandwidth under various launch conditions, can be obtained directly from Equations (5) and (6). This fiber model, in conjunction with the device models for the rest of the components of the optical link, was used to simulate the entire link. These link simulations were the basis from which the Telecommunications Industry Association, through the work of its FO-2.2.1 group, developed the specifications for the next-generation multimode fiber [14]. The primary results of these simulations are given in the section which presents the second design example.

Noise modeling

The types of noise included in the simulations and calculations of power penalties depend upon the link type (single mode, multimode fiber), laser type (VCSEL, Fabry–Perot, DFB), lasing wavelength, and link length. Here we describe two of the laser noises that are contributors to power penalties in LAN links: modal noise and mode partition noise.

Modal noise

In the early 1990s, when a shift in the data communication industry was about to occur from the use of self-pulsating, low-coherence lasers to the use of non-self-pulsating, highcoherence lasers, concerns arose regarding a potential problem due to modal noise. Previous modal noise modeling efforts had incorporated overly conservative assumptions which, if applied, would predict that modal noise would be the dominant noise source in a multimode fiber link and in most cases would prohibit error-free operation [15-17]. Practical experience with such links was contrary to the early models, and a study was begun of modal noise, resulting in an improved noise model [18] that predicted link penalties much closer to measurement and furthermore predicted that modal noise would not be the dominant noise source in multimode fiber links. This modal noise model was used in the development of the 1-Gb/s Fibre Channel standard, the 622-Mb/s ATM forum, and the IEEE 802.3z standard (also known as Gigabit Ethernet), and its predicted power penalty was eventually

incorporated into the Gigabit Ethernet Link Model spreadsheet [2]. The net result of these efforts was that modal noise could be managed by maintaining a limit on the maximum connector loss of a single connector and a limit on the maximum total loss of all connectors.

Modal noise is an additive amplitude noise that occurs when a fiber link contains a combination of a speckle pattern within the fiber, a mode-selective loss (or speckle-dependent loss), and time-varying laser and or fiber properties. If the fiber modes are changing with time, either due to fiber movement or laser changes, and there is a point in the link which selectively attenuates fiber modes (e.g., a misaligned connector), the optical amplitude varies with time beyond this point. This time variation in the amplitude is designated as *modal noise*.

A brief description of the modal noise model is included here, while a detailed description can be found in [18]. Modal noise occurs only on the optical 1s in the data pattern; hence, the BER can be calculated from the following expression, where $V_{\rm t}$ is the decision threshold, $p_{\rm grec}$ is the receiver noise pdf, $p_{\rm glfm}$ is the low-frequency Gaussian noise probability density function (pdf) of the mth connector in the link, and $p_{\rm expm}$ is the high-frequency exponential noise pdf of the mth connector in the link:

$$BER = \int_{-\infty}^{V_{t}} p_{\text{grec}} \times p_{\text{glf1}} \times p_{\text{glf2}} \times \cdots \times p_{\text{glfm}} \times p_{\text{exp1}} \times p_{\text{exp2}}$$

$$\times \cdots \times p_{\text{expm}} d\nu. \tag{7}$$

The low-frequency Gaussian noise pdf of the *m*th connector in the link is given by

$$p_{\text{glfm}}(\nu) = \frac{1}{\sigma_{\text{g}} \sqrt{2\pi}} \exp\left[-\frac{(\nu - \nu_0)^2}{2\sigma_{\text{g}}^2}\right],\tag{8}$$

where

$$\sigma_{\rm g}^2 = \frac{\gamma_{\rm l}^2 (1 - \eta)}{N \eta} \,, \tag{9}$$

and where γ_1 is the contrast of the speckle pattern in the fiber, η is the magnitude of mode-selective loss, and N is the number of fiber modes. The high-frequency exponential noise pdf of the mth connector is given by

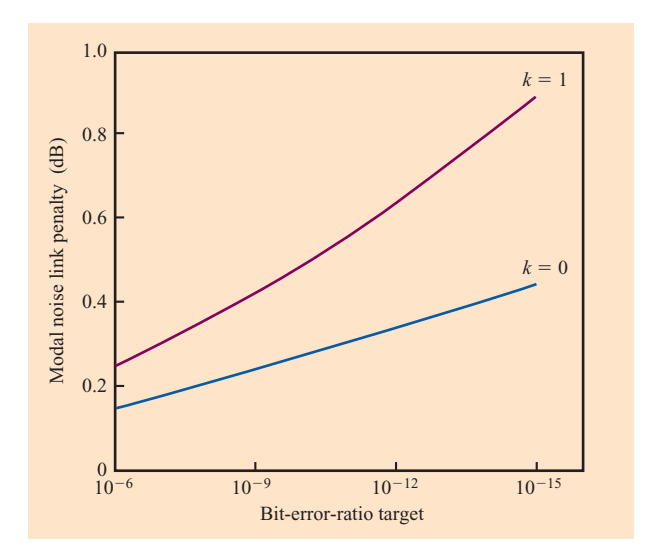
$$p_{\text{expm}}(\nu) = \frac{1}{\sigma_{\text{e}} \sqrt{2\pi}} \exp\left[-\frac{|\nu - \nu_{0}|^{2}}{2\sigma_{\text{e}}^{2}}\right], \tag{10}$$

where

$$\sigma_{\rm e}^2 = \frac{\gamma_{\rm h}^2 k^2 (1 - \eta)}{N \eta} \frac{1 - \sum_j a_j^2}{\sum_j a_j^2}$$
 (11)

231





Typical simulations (at k=0 and 1) of a worse-than-worst-case multimode fiber link (i.e., double the maximum connector loss) using only the modal noise model. This simulation predicts that the maximum penalty due to modal noise should be less than 0.6 dB.

and where γ_h is the "high-frequency" contrast of the speckle pattern in the fiber, k is the mode partition coefficient, and $\sum a_j^2$ is the variance of the relative mode power of the laser spectrum.

In summary, while the mathematical description of the modal noise model is a bit tedious, there are only six physical parameters that have to be supplied. Two of these describe the fiber: the fiber bandwidth and initial number of modes propagating. Two describe the link: the location and loss of each connector. The remaining two are related to the laser spectrum and coherence.

Figure 8 shows typical simulations of the modal noise model. Simulated in the figure is a 260-m multimode fiber link with three 0.5-dB loss connectors spaced 2 m apart at the beginning and three 0.5-dB loss connectors spaced 2 m apart at the end of the link (a worse-than-worst-case link). The six connectors were assumed to have double the maximum amount of connector loss, in accordance with the IEEE 802.3z standard. The model predicts that the modal noise penalty should be less than 0.6 dB.

Mode partition noise

It has been shown previously that the mode partition noise (MPN) can significantly affect the achievable distance in fiber optic links driven by Fabry–Perot laser diodes [19]. The mode partition noise is due to the dispersive nature of the fiber and the anticorrelation of the fluctuations of the laser modes. These fluctuations of the laser modes become larger after transmission through the fiber.

The mode partition noise and the laser linewidth are the two parameters that most affect the achievable distance of high-speed links using multimode Fabry–Perot lasers. In a dispersionless link, the mode partition noise from the laser would not cause any problems, since all modes are synchronized. However, in the presence of fiber dispersion at the other end of the fiber, the modes get out of synchronization, which causes degradation of the signal-to-noise ratio at the receiver. The mode partition theory that is widely used was first developed by Ogawa [20]. A brief description of this model is given here: Let A_i represent the power in each of the laser longitudinal modes at wavelength λ_i . Assuming that the signal at the receiver has a pulse shape f(t), the received signal can be expressed in the form

$$r(t) = \sum_{i} f(t, \lambda_i) A_i. \tag{12}$$

It has been shown that the standard deviation of the mode partition noise is given by

$$\sigma_{\rm mpn} = k \left[\sum_{i} f_i^2 \bar{A}_i - \left(\sum_{i} f_i \overline{A}_i \right)^2 \right]^{1/2}. \tag{13}$$

The mode partition noise power penalty depends on the steady-state laser spectrum A_i . Assuming a Gaussian shape for the laser spectrum, and a continuum of modes, Ogawa derived the formula for the standard deviation of the mode partition noise,

$$\sigma_{\rm mpn} = \frac{k}{\sqrt{2}} \left\{ 1 - \exp\left[-\left(\pi B L D \sigma_{\lambda}\right)^{2} \right] \right\}, \tag{14}$$

where k is the mode partition noise coefficient, which is a measure of the correlation between the modes,

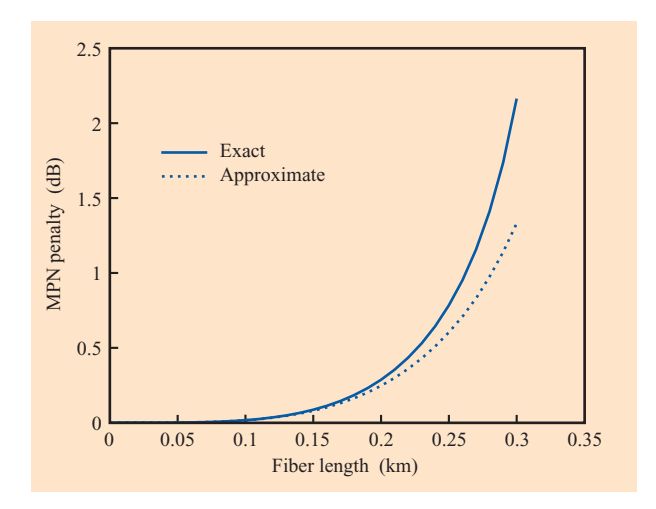
$$k^2 = \frac{\overline{A_i A_j} - \overline{A_i A_j}}{\overline{A_i A_j}}.$$
 (15)

The above expression for the MPN standard deviation has been extended in the IBM optical link simulator to the case in which intersymbol interference is present in the system. In order to find the average probability of error, one needs to know the mode partition noise standard deviation at each of the sampling points, which is accomplished by calculating Equation (13) at each bit sampling time:

$$\sigma_{\rm mpn}(nT) = k \left\{ \sum_{i} f_i^2(nT) \bar{A}_i - \left[\sum_{i} f_i(nT) \overline{A}_i \right]^2 \right\}^{1/2}, \tag{16}$$

where $f_i(nT)$ is the value of the signal waveform f at time t = nT. The total noise variances for the 1 and 0 logical level are given by

$$\sigma_1^2 = \sigma_{\text{RX},1}^2 + \sigma_{\text{rin}}^2 + \sigma_{\text{mpn}}^2(nT)$$



Comparison of the exact and the approximate formulas for a hypothetical laser having a large number (200) of modes and small mode separation (0.1 nm). The differences became larger as the penalty exceeded $0.75~\mathrm{dB}$.

and

$$\sigma_0^2 = \sigma_{\text{RX},0}^2 + \sigma_{\text{rin}}^2 + \sigma_{\text{mpn}}^2(nT),$$
 (17)

where $\sigma_{\text{RX},i}$ is the receiver thermal and shot noise standard deviation for the 1 and 0 level, and σ_{rin} is the relative intensity noise standard deviation.

Examples of design of LAN links using the IBM optical link simulator

Example 1: Effects of mode partition noise in shortwavelength multimode links

In this section, we compare the power penalties as calculated with Equation (1) using the variance found using either Equation (14) or Equation (16). Several cases are considered to illustrate the level of accuracy of the analytic approximation given in Equation (14). Laser spectrum shapes are most commonly in the forms of Gaussian and Lorentzian distributions, although simulations were also performed with an exponential distribution. Cases of very few modes and the worst case of only three laser modes are also considered.

The first example, a hypothetical laser with a large number of modes and a small mode separation, established that the approximate formula [Equation (14)] and the exact calculation [Equation (16)] give the same result for the same input parameters. In this example we assumed a large number (200) of modes closely spaced (0.1 nm) with Gaussian shape for the spectrum, so the assumption of a continuum of modes and Gaussian shape

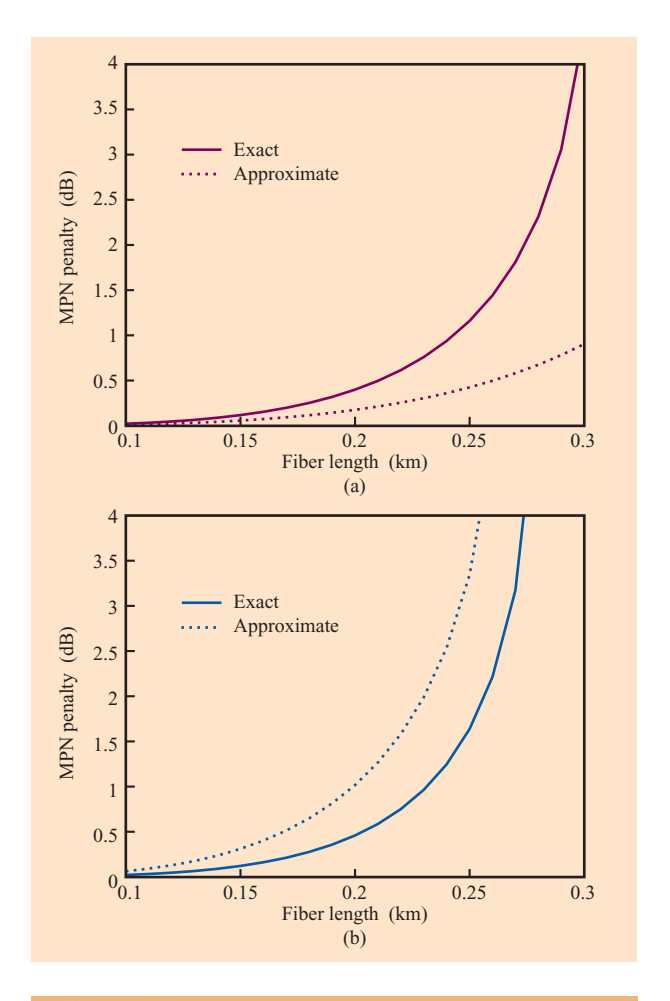


Figure 10

Comparison of approximate formula and exact calculations of mode partition noise penalty. N=3 modes were assumed, with mode separation of 1 nm for both cases. The k factor was assumed to be 0.5 at 850 nm. The results, which depend on the shape of the laser spectrum, illustrate the inconsistent predictions of the approximate mode partition noise formula. (a) Gaussian-shaped laser spectrum with rms linewidth of 0.46 nm, in which the approximate formula is optimistic; (b) Lorentzian laser spectrum with rms linewidth of 0.76 nm, in which the approximate formula is pessimistic.

was valid. Figure 9 shows the comparisons at 850 nm, where we used k = 0.5. Similar results were obtained at 1300 nm. The differences between the approximate formula and the exact calculation were larger when the penalties were larger than 0.75 dB. The differences were due to the second approximation, when the cosine (representing the signal shape) was replaced with series expansion.

The second example (**Figure 10**) shows that the approximate formula can be overly optimistic or overly pessimistic, depending on the shape of the laser spectrum.

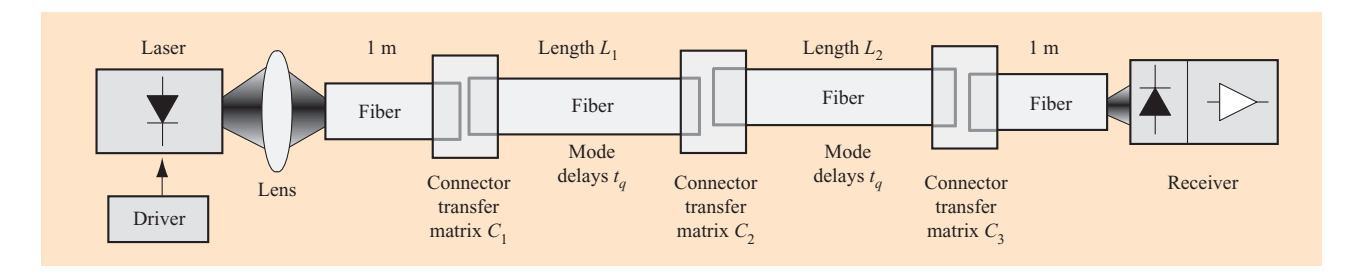


Figure 11

Elements of multimode fiber link model. The connectors have random offsets, resulting in different connector transfer matrices.

It pertains to a laser having three modes, with a mode separation of 1 nm. In the case of a Gaussian-shaped spectrum, the formula is very optimistic, predicting a penalty of only 0.8 dB at a distance of 300 m, while the exact calculation shows that the mode partition noise penalty exceeds 4 dB and approaches a floor. In the second case, the laser spectrum was assumed to have a Lorentzian shape, three laser modes, and an rms linewidth $\sigma_{\rm l}=0.76$ nm. In this case the approximate formula is pessimistic. Similar results were obtained for a 1300-nm window.

These results illustrate the inadequacy of the analytic approach to calculate the mode partition noise penalty: The shape of the spectrum, as well as the number of modes, has a sizable effect on the mode partition noise. The approximate formula does not take into account the number of modes and their distribution. As we indicated earlier, another source of errors is the approximation expansion of the cosine term in power series. These approximations lead to unpredictable results, and the use of the approximated formula may therefore lead to link failures.

Example 2: Development of the next-generation multimode fiber

An ever-increasing demand for greater information bandwidth has led to an explosion of fiber optic networks operating at gigabit speeds. There are currently efforts within the IEEE, ATM, and Fibre Channel Standard committees to develop communications standards for 10-Gb/s bit rates and beyond. In developing the communications standards, significant differences between the measured fiber bandwidth using historical overfilled launch conditions and those measured using laser launches have been found. In most cases, there was a significant increase in the fiber modal bandwidth using the laser launches; however, there were a few cases in which the

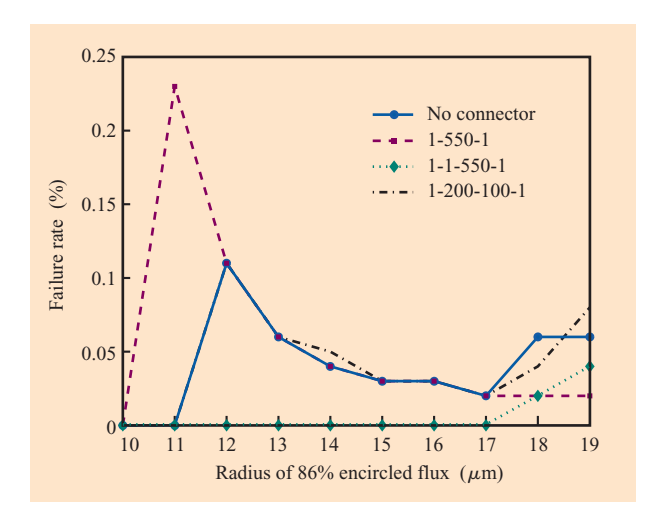
bandwidth fell below its rated value. The rated minimum bandwidth of Fiber Distributed Data Interface (FDDI)-grade fiber is 160 MHz·km at 850 nm for 62.5- μ m multimode fiber, and 500 MHz·km for 50- μ m fiber. At 10 Gb/s, this bandwidth is not sufficient to achieve 300 m on both types of multimode fiber. For example, distances shrink to 28 m for 62.5- μ m fiber at 10 Gb/s and 5–10 m at 40 Gb/s, which no longer satisfies customer needs.

To address this problem, a new high-speed multimode fiber (MMF) has been developed that has a minimum bandwidth greater than 2000 MHz·km and is capable of reaching at least 300 m with optical transceivers operating at a wavelength range of 840–860 nm. The new 50-μm MMF is now available from several fiber manufacturers. The Telecommunications Industry Association (TIA) fiber optics group FO-2.2.1, which worked for more than two years to define the fiber and laser specifications to achieve the 300-m distance target, conducted several round-robin measurements and generated the final specifications [14] for the laser and the fiber that were approved in the first half of 2002. The high data capacity is achieved by controlling both the laser launch conditions and the fiber maximum differential mode delay (DMD).

Multimode fiber link model

Elements of the multimode fiber link model are depicted in **Figure 11**. Besides the standard components found in other link block models, the multimode fiber link block model includes a block that takes into account the effect of the launch conditions on the transfer function of the fiber, as well as the degradations in each of the connectors in the link. The launch conditions at the transmitter are affected by the properties of the laser (beam spot size, number of modes, distribution of power between the modes), as well as the beam transformation by the lens. Another source of change in the launch conditions is the offset of the optical axis of the fiber and that of the laser beam entering the fiber. The offset can be attributed to either mechanical offset or tilt in the placement of the

⁴ The IEEE 802.3ae standard was approved for publication in June 2002.



Link failure rate due to exceeding ISI limit as a function of the encircled flux. Four link configurations were considered; one was a straight link without connectors and the others were labeled 1-550-1, 1-1-550-1, and 1-200-100-1. The numbers correspond to the length of each fiber section in the link. The DMD profile used in the calculations was 0.7 ps/m from 0 to 23 μ m and 0.23 ps/m from 5 to 16 μ m.

laser on the carrier, or the fiber. Independently of the origin of the offset and tilt, both introduce changes in the coupling of the laser light into the fiber modes, thereby affecting the transfer function of the fiber, and thus the performance of the link.

The offsets between the fiber and the laser and the connectors were treated in a statistical manner in the simulation, as well as the laser mode distribution and the fiber propagation times. We performed a simulation of more than 40000 links with random input parameters. For each link we calculated the ISI penalty, deterministic jitter, and retiming window, as well as the fiber bandwidth, using the approach outlined in [21]. The results obtained as a function of the DMD and laser-encircled flux are shown in Figure 12. We considered four link configurations, of which one was a straight link without connectors; the others were labeled 1-550-1, 1-1-550-1, and 1-200-100-1. The numbers correspond to the lengths of each of the fiber sections in the link. For example, the 1-200-100-1 link configuration consists of a link whose fibers are 1 m, 200 m, 100 m, and 1 m long. The laserencircled flux at a given radius (usually expressed in percent) is the fraction of the total optical power in the fiber core contained in the circle defined by that radius. An interactive program for the analysis of the data allowed "tweaking" of the fiber mask and the laserencircled flux specification to optimize cost. An overall

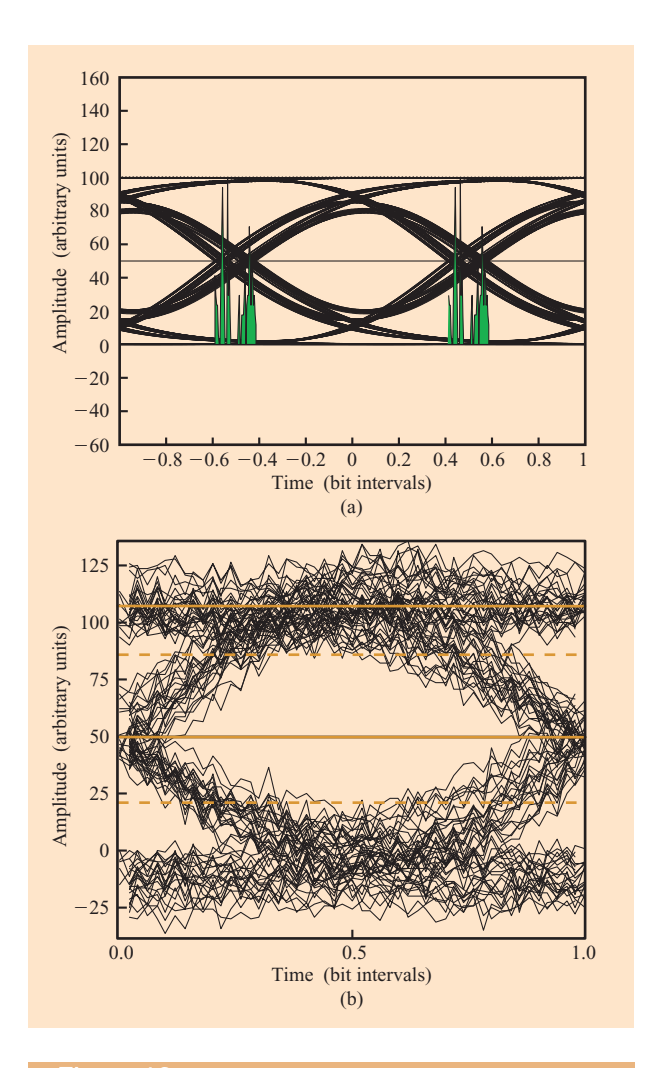


Figure 13

Eye diagrams at the output of a 1-km-long link using next-generation multimode fiber: (a) Simulated eye diagram; (b) measured eye diagram.

average link failure rate of less than 0.5% was reached when the link intersymbol interference penalty limit was used as a criterion, instead of the fiber bandwidth, which predicted that more than 1% of the links would fail in the case considered in the figure.

Prediction of 20-Gb/s link performance

We have also used the simulation tool to predict the performance of a 1-km-long link over the next generation of multimode fiber. The fiber DMD profile was flat, with maximum DMD of 0.056 ps/m, far exceeding specifications. **Figures 13(a)** and **13(b)** respectively show simulated and measured eye diagrams. The simulation predicted 2.45 dB of ISI penalty and 0.7 dB of mode partition noise penalty. In comparison, the Gaussian approximation predicts 5.5 dB

of ISI penalty and 2.5 dB of mode partition noise penalty. The simulated ISI penalty is comparable to the 2.25 dB measured ISI penalty. The usage of the advanced link modeling tool is obvious, since the Gaussian model would predict that the link would fail, while in fact the link would work with margin, as confirmed by the experimental results. Use of the advanced model would result in more accurate simulations, potentially avoiding overdesign and offering cost savings because of relaxed link parameters and better link component yield.

Concluding remarks

In this paper we have described a link-design methodology using the IBM simulation tool and device models used for simulating LAN links over multimode fibers. Experimental results have supported our performance predictions for high-speed multimode links, for which simpler models based on the Gaussian approximation predict noise floors. The IBM simulation tool has been used to support development process for three generations of Fibre Channel, ATM, and Ethernet standards, and continues to be important in the development of cost-effective specifications for both transmitter and fiber.

- *Trademark or registered trademark of International Business Machines Corporation.
- **Trademark or registered trademark of The Mathworks, Inc., or Avant! Corporation LLC, a subsidiary of Synopsys, Inc.

References

- D. Stigliani, "ESCON Fiber Optic Links," Handbook of Fiber Optic Data Communication, 2nd edition, C. DeCusatis, Ed., Academic Press, Inc., New York, 2002, Ch. 14.
- 2. M. Nowell, D. Cunningham, D. Hanson, and L. Kazovsky, "Evaluation of Gb/s Laser Based Fibre LAN Links: Review of the Gigabit Ethernet Model," *Opt. & Quantum Electron.* **32**, 169–192 (2000).
- 3. Y. M. Wong, D. J. Muehlner, C. C. Faudskar, M. Fishteyn, J. V. Gates, P. J. Anthony, G. J. Cyr, J. Choi, J. D. Crow, D. M. Kuchta, P. K. Pepeljugoski, K. Stawiasz, W. Nation, D. Engebretsen, B. Whitlock, R. A. Morgan, M. K. Hibbs-Brenner, J. Lehman, R. Walterson, E. Kalweit, and T. Marta, "Technology Development of a High-Density 32-Channel 16 Gb/s Optical Data Link for Optical Interconnection Applications for the Optoelectronic Technology Consortium," J. Lightwave Technol. 13, No. 6, 995–1016 (June 1995).
- B. K. Whitlock, P. K. Pepeljugoski, D. M. Kuchta, J. D. Crow, and S. M. Kang, "Computer Modeling and Simulation of the Optoelectronic Technology Consortium (OETC) Optical Bus," *IEEE J. Sel. Areas Commun.* 15, No. 4, 717–730 (1997).
- P. K. Pepeljugoski, B. K. Whitlock, D. M. Kuchta, J. D. Crow, and S.-M. Kang, "Modeling and Simulation of the OETC Optical Bus," *IEEE LEOS '95 Conference Proceedings*, San Francisco, October 31, 1995, Vol. 1, Paper OIPS3.2, pp. 185–186.
- B. K. Whitlock, J. J. Morikuni, E. Conforti, and S. M. Kang, "Simulating Optical Interconnects," *IEEE J. Circuits & Dev.* 11, No. 3, 12–18 (May 1995).

- G. P. Agrawal and N. K. Dutta, Long Wavelength Semiconductor Lasers, Van Nostrand Reinhold, New York, 1986.
- R. S. Tucker and D. J. Pope, "Circuit Modeling of the Effect of Diffusion on Damping in a Narrow-Strip Semiconductor Laser," *IEEE J. Quantum Electron.* QE-19, No. 7, 1179–1183 (July 1983).
- 9. D. M. Byrne and B. A. Keating, "A Laser Diode Model Based on Temperature Dependent Rate Equations," *IEEE Photon. Technol. Lett.* **PTL-1,** 356 (1989).
- IEEE Photon. Technol. Lett. PTL-1, 356 (1989).
 10. R. S. Tucker, "Large-Signal Circuit Model for Simulation of Injection-Laser Modulation Dynamics," IEE Proc. 128, Pt. I, 180–185 (1981).
- D. M. Kuchta, P. Pepeljugoski, and Y. Kwark, "VCSEL Modulation at 20 Gb/s Over 200 m of Multimode Fiber Using a 3.3 V SiGe Laser Driver IC," Technical Digest of the LEOS Summer Topical Meetings, 2001, Paper WA2.1.
- D. Marcuse, "Gaussian Approximation of the Fundamental Modes of Graded-Index Fibers," J. Opt. Soc. Amer. 68, No. 1, 103–109 (January 1978).
- I. A. White and S. C. Metler, "Modal Analysis of Loss and Mode Mixing in Multimode Parabolic Index Splices," *Bell Syst. Tech. J.* 62, No. 5, 1189–1207 (1983).
- "Detail Specification for 850-μm Laser-Optimized 50-μm Core Diameter/125-μm Cladding Diameter Class Ia Graded-Index Multimode Optical Fibers," TIA/EIA-492AAAC, Telecommunication Industry Association.
- M. J. Lum, D. M. Fuller, A. Hadjifotiou, and R. E. Epworth, "Modulation-Induced Modal Noise in Digital Systems—the Prediction and Measurement of Bit Error Ratio," Proceedings of the Tenth European Conference on Optical Communications, September 1984, pp. 240–241.
- T. Kanada, "Evaluation of Modal Noise in Multimode Fiber-Optic Systems," *IEEE J. Lightwave Technol.* LT-2, No. 1, 11–18 (February 1984).
- 17. A. M. J. Koonen, "Bit-Error-Rate Degradation in a Multimode Fiber Optic Transmission Link Due to Modal Noise," *IEEE J. Sel. Areas Commun.* SAC-4, No. 9, 1515–1522 (December 1986).
- R. J. S. Bates, D. M. Kuchta, and K. P. Jackson, "Improved Multimode Fibre Link BER Calculations Due to Modal Noise and Non-Self-Pulsating Laser Diodes," Opt. & Quantum Electron. 27, No. 4, 203–224 (April 1995).
- G. P. Agrawal, "Dispersion Penalty for 1.3 μm Systems with Multimode Semiconductor Lasers," *IEEE J. Lightwave Technol.* 6, No. 5, 620–625 (May 1988).
- K. Ogawa, "Semiconductor Laser Noise: Mode Partition Noise," Semiconductors and Semimetals, Academic Press, Inc., New York, Vol. 22, Part C, Chapter 8, pp. 299–330.
- P. K. Pepeljugoski, D. M. Kuchta, Y. Kwark, P. Pleunis, and G. Kuyt, "15.6 Gb/s Transmission Over 1 km of Next Generation Multimode Fiber," *IEEE Photon. Technol. Lett.* 14, No. 5, 717–719 (May 2002).

Received March 4, 2002; accepted for publication August 9, 2002

Petar K. Pepeljugoski IBM Research Division, Thomas J. Watson Research Center, P.O. Box 218, Yorktown Heights, New York 10598 (petarp@us.ibm.com). Dr. Pepeljugoski is a Research Staff Member in the Communication Technology Department at the IBM Thomas J. Watson Research Center. He received his B.S. degree from the Ss. Cyril and Methodius University in Skopje, Macedonia, in 1982, his M.S. degree from the University of Belgrade in 1986, and his Ph.D. degree from the University of California at Berkeley in 1993. In 1994 he joined IBM, where his research work has included design, modeling, and characterization of high-speed multimode fiber LAN links and parallel interconnects. His modeling tools were used by the Telecommunication Industry Association (TIA) in the development of the next-generation fiber. In 2003 he received a Certificate of Appreciation from the TIA for this work. In 2002, he received an IEEE Recognition Award for his contributions to the development of the IEEE 10-Gigabit Ethernet Standard. Dr. Pepeljugoski is an author or a coauthor of more than 30 technical papers; he is a member of the Institute of Electrical and Electronics Engineers.

Daniel M. Kuchta IBM Research Division, Thomas J. Watson Research Center, P.O. Box 218, Yorktown Heights, New York 10598 (kuchta@us.ibm.com). Dr. Kuchta is a Research Staff Member in the Communication Technology Department at the IBM Thomas J. Watson Research Center. He received B.S., M.S., and Ph.D. degrees in electrical engineering and computer science from the University of California at Berkeley in 1986, 1988, and 1992, respectively. He subsequently joined IBM at the Thomas J. Watson Research Center, where he has worked on high-speed VCSEL characterization, multimode fiber links, and parallel fiber optic link research. Dr. Kuchta is an author or coauthor of nine patents and more than 25 technical papers; he is a Senior Member of the Institute of Electrical and Electronics Engineers.